

Energy Relaxation of Photoexcited Hot Electrons in GaAs^{†*}

R. Ulbrich[†]

Physikalisches Institut der Universität Frankfurt, Frankfurt am Main, Germany

(Received 21 June 1973)

The energy relaxation of an initially hot photoexcited free-electron population has been investigated in high-purity GaAs at lattice temperatures $T_L = 2$ to 4 K. The electron energy distribution function $f(E)$ was determined directly from the line shape of the conduction-band-acceptor luminescence. Two different experiments—transient and steady state—were performed: (i) the time development of $f(E)$ in the electron energy range $0 \leq E \leq 8$ meV was measured with subnanosecond time resolution after excitation with short light pulses (≈ 0.2 nsec, $\hbar\omega = 1.92$ eV) and (ii) the steady-state dependence of $f(E)$ on cw-excitation-light power was measured. The experimental results are compared with theoretical energy relaxation rates using the known standard electron-phonon scattering mechanisms. In the electron temperature range above ≈ 16 K both experiments indicate higher energy-loss rates than expected theoretically. At lower electron temperatures good agreement with theory is obtained. It is shown that interelectronic collisions effectively randomize the electron energies during the relaxation process even for the low electron densities (n_e as low as 2×10^{11} cm⁻³) achieved in the experiments.

I. INTRODUCTION

The energy relaxation of a nonequilibrium distribution of free carriers in a semiconductor occurs via interaction of the electrons with lattice vibrations^{1,2} and, under suitable conditions, also by scattering with neutral impurities ("impact ionization")³ and ionized impurities ("capture").⁴ Interelectronic collisions redistribute energy and momentum among the carriers, but do not change the total energy of the distribution. If the carrier density is high enough, $e-e$ ($h-h$) collisions dominate and we find separate thermal distributions of electrons and holes with temperatures T_e and T_h that can be substantially higher than the lattice temperature T_L .⁵

In a typical III-V semiconductor such as GaAs the relevant electron-one-phonon scattering processes are polar-optical, piezoelectric, and acoustical-deformation-potential scattering.^{1,2,6} The related scattering rates form the basis for the investigation of carrier transport as a function of electric field strength and temperature.^{6,7} Most experiments have dealt with the electric field and temperature dependence of drift and Hall mobilities,^{1,7} and in only a few experiments have actual carrier distribution functions been measured directly. Thermalization of carriers has been studied earlier in photoluminescence experiments in InSb.⁸ Electron- and hole-velocity distributions have been determined by light-scattering experiments in GaAs.⁹ Shah and Leite have measured the carrier temperature (assuming $T_e = T_h$) as a function of excitation power in a cw photoluminescence experiment by analyzing the high-energy tail of band-to-band emission in GaAs.¹⁰ Using the same method, Southgate *et al.* have studied the heating of the electron distribution by an applied

electric field.¹¹

In the present work we investigate in a fairly direct way the effect of electron-phonon scattering processes and interelectronic collisions on the energy relaxation of photoexcited hot electrons in GaAs. The paper describes the first measurement of the time development of the electron distribution function after pulsed photoexcitation (with subnanosecond light pulses) of electrons high in the conduction band. The electron energy distribution function $f(E)$ is determined from the line shape of the conduction-band-acceptor luminescence (e, A^0), which is an accurate and inherently fast probe for $f(E)$ in the electron energy range $0 \leq E \leq 15$ meV. By the same probing method we have measured the steady-state heating of the photoexcited electron distribution as a function of cw-excitation-light power. Both experiments—transient and steady state—enable us to make quantitative comparisons with theory, based on (i) the energy dependence of the power losses by electron-phonon scattering and (ii) the power-balance equation.

Section II contains a description of the experimental method and the sample properties. Section III deals with the energetic and spatial distributions of electrons immediately after the optical excitation. The experimental results, i. e., $f(E)$ as a function of time and $f(E)$ as a function of excitation-light power, are given in Sec. IV, together with a discussion of the accuracy and usefulness of the probing method. Finally, Sec. V contains a comparison of our experimental results with theoretical energy relaxation rates, calculated from the known electron-one-phonon scattering rates with parameters appropriate to the experimental conditions. The results are summarized in Sec. VI.

II. EXPERIMENTAL METHOD AND SAMPLE PROPERTIES

For the pulsed photoexcitation of hot electron-hole pairs we used a mode-locked cw Kr-ion laser with 100-mW average output power at $\hbar\omega = 1.916$ eV, emitting ~ 0.2 -nsec-wide light pulses with 9.6-nsec pulse spacing.¹² Single light pulses were selected out of the continuous pulse train with a synchronized optical gate (LiNbO₃ Pockels cell). Considering all losses in the gate, filters, and windows, and taking the reflectivity at the sample surface as 0.32, the sample was excited by light pulses with 2×10^{-11} -J energy content (corresponding to 6×10^7 photons) and repetition rates up to 3×10^4 Hz.

The high-purity epitaxial GaAs samples with smooth as-grown surfaces were immersed in liquid helium which could be pumped. The sample properties are listed in Table I. We estimate the rise in lattice temperature due to heating by the excitation light to be negligible in the range of excitation powers reported here. Even at the highest cw power density (60 W/cm²), the energetic position of the near-band-edge bound-exciton lines did not shift within experimental accuracy (0.03 meV): This implies that the lattice temperature change was less than 3 K in the worst case.

The sample luminescence was collected with a $f:1.5$ optical system, dispersed by a 0.75-m grating spectrometer and detected with an RCA C31000E photomultiplier. We used a single-photon timing arrangement similar to that described by Bachrach¹³ to measure the time dependence of the luminescence. The over-all time-resolving capability of the system is characterized by a measured prompt-response curve of Gaussian shape with a full width at half-maximum (FWHM) of 0.8 nsec, corresponding to a time resolution (standard deviation) less than 0.4 nsec. The illumination of the photomultiplier cathode was always kept so low (≤ 0.01 counts per excitation pulse on the average) that pileup effects could not affect the results.¹⁴

The cw photoluminescence measurements were performed with the same Kr-ion laser emitting

200-mW unmodulated power at $\hbar\omega = 1.916$ eV. By means of neutral-density filters the excitation-light power density was varied between 1×10^{-4} and 6×10^1 W/cm². The spectra were taken by the conventional lock-in technique and were recorded continuously. All luminescence spectra were corrected for the spectral sensitivity of the detection system.

III. ENERGETIC AND SPATIAL DISTRIBUTION OF PHOTOEXCITED ELECTRONS

In the region of k space covered by our experiments ($|\vec{k}| \leq 8 \times 10^6$ cm⁻¹) the lowest conduction band and the upper valence bands of GaAs are described by

$$E_c(\vec{k}) = \frac{\hbar^2 k^2}{2m_0} + \frac{E_g}{2} \left[\left(1 + \frac{4E_p \hbar^2 k^2}{E_g^2 2m_0} \right)^{1/2} - 1 \right], \quad (1)$$

$$E_v(\vec{k}) = \frac{\hbar^2}{2m_0} \{ A k^2 \pm [B^2 k^4 + C^2 (k_x^2 k_y^2 + k_y^2 k_z^2 + k_z^2 k_x^2)]^{1/2} \}, \quad (2)$$

where m_0 is the free-electron mass, E_g the band-gap energy, $2E_p/m_0$ the interband matrix element, and A, B, C the set of valence-band parameters.^{15,16} We adopted values for A, B, C given by Lawaetz¹⁷ (see Table II). A careful analysis of luminescence excitation spectra exhibiting oscillatory structure due to successive LO-phonon emission¹⁸ yields an average "optical" heavy-hole mass $\langle m_{hh}^* \rangle_{opt} = 0.57m_0$ which is consistent with this set of parameters.¹⁹

For our given photon energy $\hbar\omega = 1.916$ eV, dipole transitions occur across the band gap from the upper valence bands [heavy- and light-hole band, Eq. (2)] and also from the split-off valence band separated by $\Delta \cong 0.34$ eV at $k=0$. Assuming a \vec{k} -independent transition-matrix element, the ratios of transitions from the heavy-hole, light-hole, and split-off valence band to the conduction band are given essentially by the density-of-states ratios 0.58 : 0.29 : 0.13. From now on we concentrate on transitions starting in the heavy-hole band and neglect the contributions from the other valence bands. Due to the warping of the heavy-

TABLE I. Properties of the high-purity epitaxial GaAs samples used in the present experiments.

Sample	Type	$ N_D - N_A $ (cm ⁻³)	N_A (cm ⁻³)	$\mu(77$ K) (cm ² /V sec)	$\mu(300$ K) (cm ² /V sec)
a	<i>n</i>	1.8×10^{12}		1.7×10^5	6×10^3
b	<i>n</i>	1.8×10^{13}	1.0×10^{14}	1.48×10^5	
c	<i>n</i>	2.0×10^{13}	2.6×10^{14}	1.02×10^5	
d	<i>p</i>	3.5×10^{13}	$\sim 1 \times 10^{14}$	9.7×10^3 ^a	4.4×10^2
e	<i>p</i>	1.4×10^{14}	$\sim 4 \times 10^{14}$	9.2×10^3 ^a	4.4×10^2
f	<i>p</i>	5.3×10^{14}	$\sim 1 \times 10^{15}$	8.9×10^3 ^a	4.5×10^2

^aNote that samples d-f are *p*-type samples.

TABLE II. Parameters used for the characterization of GaAs ($T=0$).

E_g	1.5192 eV ^a	$\hbar\omega_{LO}$	36.74 meV ^b
m_e^*	0.0665 m_0 ^c	κ_∞	10.63 ^d
$A, B, C $	-7.65, -4.82, 7.71 ^e	κ_0	12.56 ^d
$\langle m_{th}^* \rangle_{opt}$	0.57 ^f	e_{14}	$4.8 \times 10^4 \text{ cm}^{-1/2} \text{ g}^{1/2} \text{ sec}^{-1}$ ^g
$2E_p/m_0$	21.3 eV ^h	E_i	7 eV ⁱ
E_A	26.9 meV ^j	ρ	5.36 g cm ⁻³ ^k
E_D	5.8 meV ^d		

^aD. D. Sell, Phys. Rev. B **6**, 3750 (1972); D. E. Hill, Solid State Commun. **11**, 1187 (1972).

^bA. Mooradian and G. B. Wright, Solid State Commun. **4**, 431 (1966).

^cH. R. Fetterman, D. M. Larsen, G. E. Stillman, P. E. Tannenwald, and J. Waldman, Phys. Rev. Lett. **26**, 975 (1971).

^dG. E. Stillman, D. M. Larsen, C. M. Wolfe, and R. C. Brandt, Solid State Commun. **9**, 2245 (1971).

^eReference 17.

^fReference 19.

^gG. Arlt and P. Quadflieg, Phys. Status Solidi A **25**, 323 (1968).

^hChosen to give m_e^* at $k=0$ in Eq. (1).

ⁱAs quoted in Ref. 6.

^jObtained from a comparison of (e, A^0) emission spectra with the theoretical line shape, Eq. (5).

hole energy surface, the initial electron energy for transitions with given

$$\hbar\omega - E_g = E_c(\vec{k}) - E_v(\vec{k}) \quad (3)$$

depends on the direction of \vec{k} . Hence the absorption of monoenergetic photons creates a broadened distribution of electron (hole) energies in the conduction (valence) band. By solving Eq. (3) for E_c and averaging over the directions of \vec{k} with the inclusion of the interband dipole-matrix element,¹⁵ we find the center of the photoexcited electron distribution in the conduction band at $\langle E_c \rangle_t = 348$ meV in our specific case, with a width of 21 meV. This electron distribution in the conduction band represents the "initial state" of the intraband energy relaxation process we are interested in.

The spatial distribution of excited carriers in the crystal is given by the intensity profile of the exciting light: From the absorption constant $\alpha(1.92 \text{ eV}) = 3.5 \times 10^4 \text{ cm}^{-1}$ a light penetration depth of $\sim 0.3 \mu\text{m}$ results.²⁰ However, for an estimate of the initial electron concentration in the transient experiment we have to consider that the light-pulse duration (~ 0.2 nsec) is much longer than the LO-phonon scattering time ($\tau_{op} \approx 4$ psec at $\langle E_c \rangle_t \approx 10\hbar\omega_{LO}$).² While emitting LO phonons the electrons diffuse to a depth of

$$l_{diff} \approx \left(\frac{\langle E_c \rangle_t}{\hbar\omega_{LO}} \right)^{1/2} l_{op}, \quad (4)$$

where $l_{op} = (2E/m_e^*)^{1/2} \tau_{op}(E)$ is the mean free path between polar-optical scattering events.²¹ Using

a suitably averaged l_{op} we find $l_{diff} \approx 6.5 \mu\text{m}$. The excitation light pulse was focused into an area 0.5×2 mm. Thus our maximum electron concentration during pulsed excitation is $n_e = 9 \times 10^{12} \text{ cm}^{-3}$.

IV. RESULTS AND DISCUSSION

To illustrate the method of determining the electron distribution function a typical cw photoluminescence spectrum is shown in Fig. 1 on a logarithmic scale. In our high-purity samples (see Table I) the conduction band-acceptor and the donor-acceptor luminescence bands are well separated and a quantitative line-shape analysis is possible.²² The (e, A^0) emission line shape $J(\hbar\omega)$ is given essentially by the product of $f(E)$ with the electron density of states $\mathfrak{N}(E)$ ^{23,24}:

$$J(\hbar\omega) \propto f(E_c) \mathfrak{N}(E_c) |M_{c,A}(\vec{k})|^2, \quad (5)$$

$$E_c = \hbar\omega - E_g + E_A.$$

$M_{c,A}(\vec{k})$ is a dipole-matrix element and E_A is the acceptor binding energy. $\mathfrak{N} \propto E_c^{1/2}$ and the energy dependence of $M_{c,A}$ is known.^{23,24} Thus we readily obtain the distribution function $f(E)$ from the (e, A^0) emission line shape by use of Eqs. (5).

It is essential for this method of probing $f(E)$ that the (e, A^0) emission be clearly separated from the related pair band (D^0, A^0) and also from emission due to other recombination centers. For this reason the method is restricted to relatively pure samples with low donor concentrations. In time-resolved measurements the time-dependent ener-

gy position of the (D^0, A^0) emission band has to be considered.²⁵ Another source of background luminescence in the energy region of interest is due to two-hole transitions originating in the radiative decay of bound excitons (A^0, X) .²⁶ This extra line, a well-defined doublet peak at $\hbar\omega = 1.4939$ eV, occurred only at higher cw excitation intensities (≥ 5 W/cm²) and could easily be corrected for in the evaluation of the spectra. The energy range within which $f(E)$ could be measured was limited at higher energies ($E_c \geq 15$ meV) by a broad background luminescence related to the partial Auger decay of (D^0, X) bound-exciton complexes.²⁷ At high excitation intensities (corresponding to the upper limit of excitation power reported here in the cw experiments) the low-energy tail of these Auger replicas²⁷ at 1.510 eV extended down to ~ 1.502 eV and masked partially the high-energy tail of the (e, A^0) emission. Both sources of background luminescence were *not* effective in the time-resolved experiment because of the much lower excitation power involved there. In the cw spectra care was taken to account for both effects when it was necessary. Distortions of the experimentally observed (e, A^0) line shape due to reabsorption were negligible: With a neutral acceptor concentration $N_A = 10^{14}$ cm⁻³ one finds absorption constants $\alpha = 0.3$ cm⁻¹ at $E_c = 20$ meV from Dumke's calculations.²⁴

Figure 2 shows the distribution function $f(E)$ de-

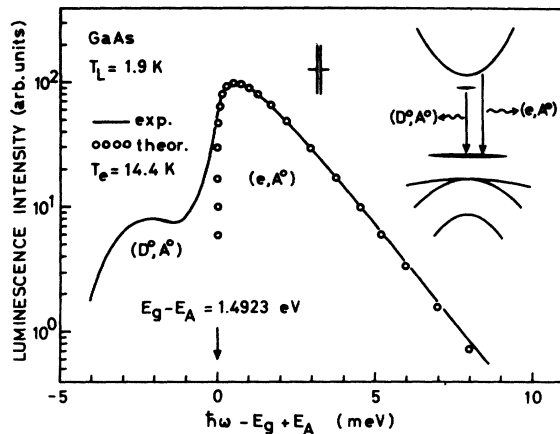


FIG. 1. Typical cw photoluminescence spectrum (solid line, logarithmic plot) showing conduction-band-acceptor (e, A^0) and donor-acceptor (D^0, A^0) emission bands clearly separated in high-purity epitaxial GaAs with one residual shallow acceptor level at $E_A = 26.9$ meV. The excitation-light power density is 6 W/cm², lattice temperature $T_L = 1.9$ K. Open circles: theoretical line shape for a thermal electron distribution with temperature $T_e = 14.4$ K. The inset shows schematically the origin of the (e, A^0) emission and its connection with the electron energy distribution in the conduction band.

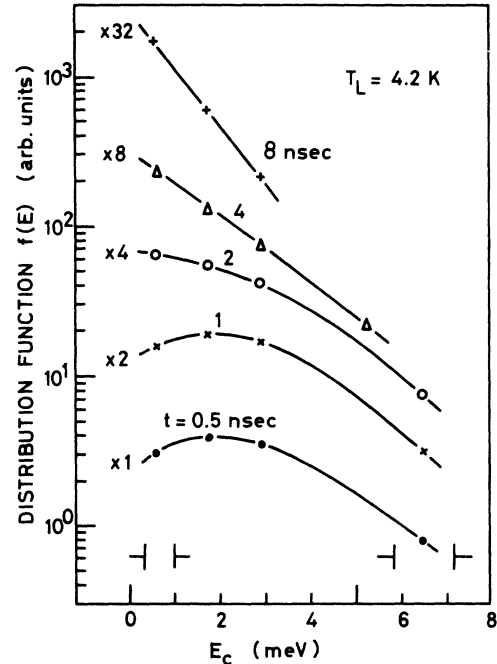


FIG. 2. Electron energy distribution function $f(E)$ at different times t after the photoexcitation of hot electrons at $t=0$ with a 0.2-nsec light pulse. $f(E)$ was determined from time-resolved measurements of the (e, A^0) emission line shape. For clarity the curves are shifted vertically by the factors indicated at left.

termined from the (e, A^0) emission line shape in the way described above, at different times after the pulsed excitation at $t=0$ (for clarity the curves are shifted vertically by the factors indicated). At times greater than ~ 2 nsec the experimental distribution turned out to be a thermal (Maxwellian) one, described by $f(E) \propto e^{-E/kT_e}$ within experimental error. From these measured distribution functions the average electron energy was found by equating

$$\langle E \rangle = \left(\int_0^\infty dE E^{3/2} f(E) \right) \left(\int_0^\infty dE E^{1/2} f(E) \right)^{-1}, \quad (6)$$

which yields, of course, in the case of the Maxwellian distributions with temperatures T_e the average energy $\langle E \rangle = \frac{3}{2} kT_e$. The average electron energy as a function of time after pulsed excitation at $t=0$ is shown in Fig. 3 (open circles).

In our second experiment the distribution function was determined as a function of the cw-excitation-light power P . A careful analysis of the (e, A^0) emission line shape with the aid of Eq. (5) revealed that $f(E)$ in all cases could be described accurately by a Maxwell-Boltzmann distribution. This result is a consequence of the relatively long free-electron lifetime of the order of 10^{-7} sec encountered in the present experiments.^{18,28} This time, of course, is sufficient to randomize the

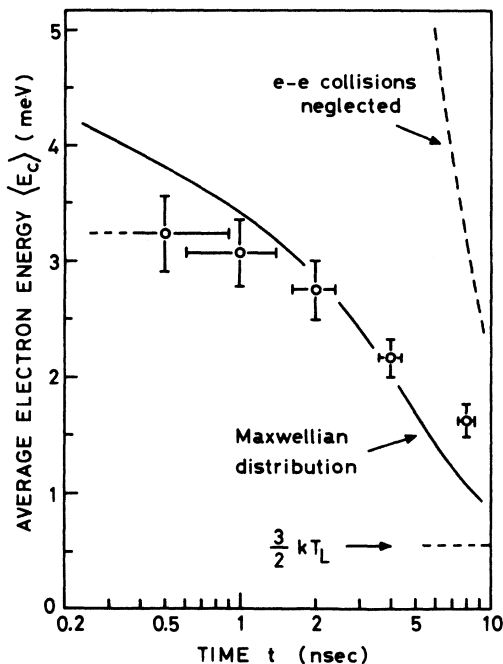


FIG. 3. Average energy $\langle E_c \rangle$ of the electron distribution as a function of time after pulsed photoexcitation at $t=0$ (open circles). The theoretical dependence of $\langle E_c \rangle$ on t (taking into account the standard electron-phonon scattering processes) is shown for two limiting cases: (i) $e-e$ collisions dominate; i.e., the distribution is Maxwellian (solid line); (ii) $e-e$ collisions are neglected (dashed line).

electron distribution perfectly via $e-e$ collisions even in our low-electron-concentration limit. The result of the cw experiment, T_e as a function of absorbed excitation power density P , is shown in Fig. 4, where the right-hand ordinate scale (in W/cm^2) gives the measured value of P , whereas the left-hand scale represents the average power per electron transferred to the randomized electron distribution, derived from a relation given in Sec. V below. For clarity the results of only two samples are shown. The other samples generated similar curves.

V. COMPARISON WITH THEORETICAL RELAXATION RATES

In this section we first calculate the average energy of the photoexcited electron population as a function of time on the basis of the standard electron-phonon scattering processes (transient case). Energy relaxation via impact ionization of neutral donors is treated briefly to illustrate its possible significance in n -type samples. Next, from the energy dependence of the different scattering mechanisms we infer by use of the power-balance equation the dependence of the mean carrier energy on

the excitation-light power (steady-state case). The experimental results of Sec. IV are then compared with the calculations.

Because it is difficult to incorporate $e-e$ scattering in a simple manner into the calculation of the transient energy relaxation, we consider for simplicity only two limiting cases where we assume that (a) $e-e$ scattering occurs much more frequently than all acoustic phonon processes together; more precisely, the average rate of energy loss to the acoustic phonons at a given electron energy is always smaller than the energy exchanged during $e-e$ collisions. Consequently, the electron distribution is a thermal one, characterized by $f(E) \propto e^{-E/kT_e}$ ²⁸; (b) $e-e$ scattering is less frequent than the acoustic phonon processes. It is evident that the latter assumption is not justified in the low-electron-energy range ($E_c \leq 3$ meV), since the steady-state experiments proved that the electron distributions were always thermal distributions, even at the lowest excitation rate corresponding

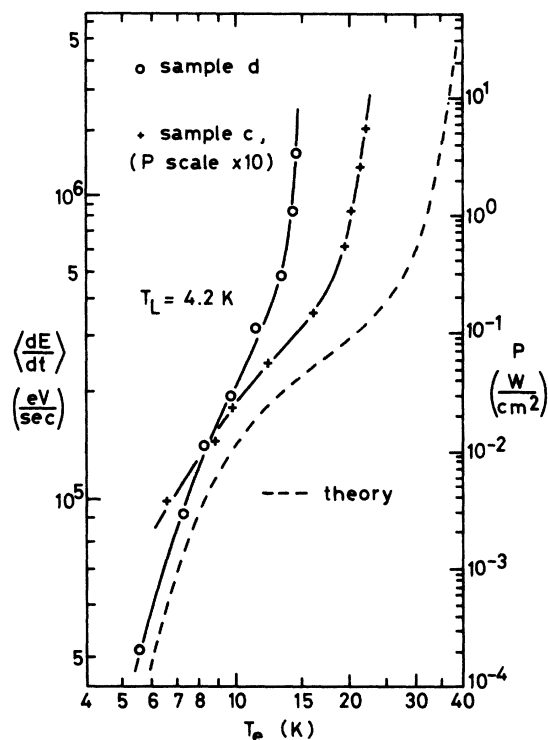


FIG. 4. Electron temperature T_e as a function of absorbed excitation light power P (right-hand ordinate scale), as measured in the cw experiments (solid lines). The left-hand ordinate scale gives the average power per carrier, $\langle dE/dt \rangle$, transferred to the randomized electron distribution. For comparison, the theoretical energy-loss rate is shown for a lattice temperature $T_L = 4.2$ K (dashed line). Note that the relation between $\langle dE/dt \rangle$ and P is not linear, as defined by Eqs. (11)–(13) (see Sec. VB).

to electron concentrations of $n_e \approx 2 \times 10^{11} \text{ cm}^{-3}$. Nevertheless, case (b) is considered to demonstrate the importance of e - e collisions even under conditions of very low electron density.

A. Mean Carrier Energy as Function of Time: Transient Case

To obtain the theoretical average carrier energy as a function of time we proceed as follows: The energy-loss rate per electron is known for each individual scattering process.^{2,30} The different loss rates are added and averaged over the Maxwellian distribution considered in case (a). This average energy-loss rate is then integrated to give the average electron energy as a function of time.

The three important averaged energy-loss rates $\langle dE/dt \rangle$ per electron in a Maxwellian distribution of temperature T_e are^{2,30}

$$\left\langle \frac{dE}{dt} \right\rangle_{\text{op}} = - (2m_e^*)^{1/2} (\hbar\omega_{\text{LO}})^{3/2} \left(\frac{q_e}{\hbar} \right)^2 (\kappa_\infty^{-1} - \kappa_0^{-1}) \times \left[\exp\left(-\frac{\hbar\omega_{\text{LO}}}{kT_e}\right) - \exp\left(-\frac{\hbar\omega_{\text{LO}}}{kT_L}\right) \right], \quad (7)$$

$$\left\langle \frac{dE}{dt} \right\rangle_{\text{pe}} = - \left(\frac{64\pi^{1/2} q_e^2 e_{14}^2 m_e^* 3/2 a (kT_e)^{1/2}}{2^{1/2} \hbar^2 \kappa_0^2 \rho} \right) \left(\frac{T_e - T_L}{T_e} \right), \quad (8)$$

$$\left\langle \frac{dE}{dt} \right\rangle_{\text{ac}} = - \left(\frac{(8)(2)^{1/2} E_1^2 m_e^* 5/2 (kT_e)^{3/2}}{\pi^{3/2} \hbar^4 \rho} \right) \left(\frac{T_e - T_L}{T_e} \right). \quad (9)$$

The subscripts op, pe, and ac denote polar-optical, piezoelectric, and acoustic-deformation-potential scattering, respectively. m_e^* is the effective electron mass, $\hbar\omega_{\text{LO}}$ the LO-phonon energy at $k \approx 0$, q_e the electronic charge, κ_∞ and κ_0 are the high- and low-frequency dielectric constants, e_{14} is the piezoelectric coupling constant, a is a dimensionless factor ~ 0.4 ,³⁰ ρ is the density of the crystal, and E_1 is the deformation-potential constant. Equations (7)–(9) describe the unscreened interactions.

Figure 5 shows the theoretical results: the total average power loss per carrier $\langle dE/dt \rangle$ versus T_e (solid line) and the contributions of the specific processes acting alone. The steep increase of $\langle dE/dt \rangle$ above $T_e \sim 32 \text{ K}$ is due to the onset of polar scattering suffered by carriers in the high-energy tail of the distribution with energies $E > \hbar\omega_{\text{LO}}$. Below 32 K the main contribution to $\langle dE/dt \rangle$ comes from piezoelectric scattering. The parameters used in the calculations are given in Table II.

In Fig. 5 we have also plotted the power loss due to impact ionization of neutral donors (dotted line). It is given by

$$\left\langle \frac{dE}{dt} \right\rangle_{\text{imp}} = - \frac{\pi^{3/2} N_D \sigma_0 E_D (kT_e)^{1/2}}{(2m_e^*)^{1/2}} \exp\left(-\frac{E_D}{kT_e}\right), \quad (10)$$

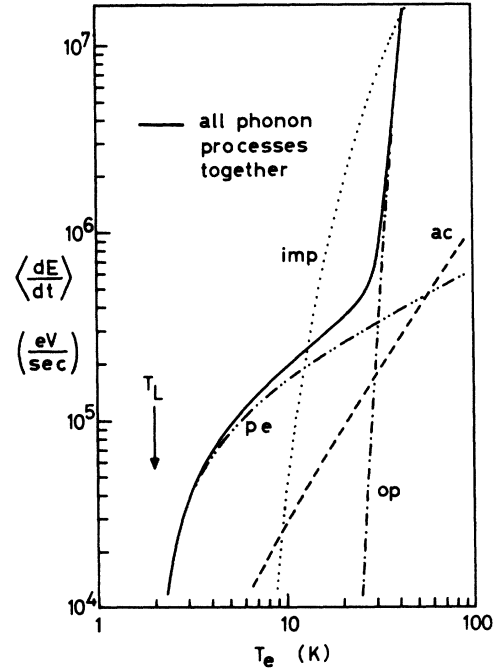


FIG. 5. Theoretical average energy-loss rate per electron, $\langle dE/dt \rangle$, for a thermal (Maxwell-Boltzmann) distribution with electron temperature T_e . The different curves denote the specific contributions from the relevant electron-one-phonon scattering processes: op—polar-optical, pe—piezoelectric, and ac—acoustic-deformation potential scattering. The full line denotes the total power loss to the lattice. For comparison the contribution due to impact ionization of neutral donors of concentration $N_D = 10^{14} \text{ cm}^{-3}$ is shown (dotted curve).

where N_D is the concentration of neutral donors with binding energy E_D and σ_0 is the cross section for impact ionization³ (taken to be constant above threshold $E \geq E_D$, $\sigma_0 = \pi a_0^2$). In n -type samples where neutral donors exist in equilibrium, this energy relaxation process could be effective in the transient experiments. The situation is complicated, however, because of the varying neutral-donor concentration during the relaxation process. To simplify the interpretation of the transient experiment we present only results obtained from p -type samples. In the cw experiments no significant difference in the relaxation behavior of electrons in n - and p -type crystals could be found.

The average energy loss for case (b), i.e., neglecting interelectronic collisions, has been found by calculating numerically the time development of the electron distribution function. Because of the threshold energy for polar optical scattering it is clear that in the energy range below $\hbar\omega_{\text{LO}}$ the assumption of a nonrandomized (i.e., nearly monoenergetic) distribution always leads to significantly smaller energy-loss rates than that obtained with

a thermal distribution. The result of the calculations, the average energy $\langle E_c \rangle$ as a function of time, is shown in Fig. 3 (solid line: Maxwell-Boltzmann distribution; dashed line: interelectronic collisions neglected, no energy randomization). It was assumed that the distribution is injected at $t=0$ with a mean energy $\langle E_c \rangle(t=0) = 17$ meV. This is justified because the initial LO-phonon emission "cascade" is run through in times very short compared with the time scale accessible to our experiments (see also Sec. V B below).

In comparing the calculated time dependence of $\langle E_c \rangle$ with the experimental results of Sec. IV (see Fig. 3) we find the following: The inclusion of $e-e$ collisions and their effective energy randomization even at low electron concentrations ($n_e < 8 \times 10^{12}$ cm $^{-3}$ in the transient experiment) is absolutely necessary to explain the fast energy relaxation which is observed. The theoretical results for the (nearly monoenergetic) distribution obtained by neglecting interelectronic collisions disagree considerably with the transient experiment (Fig. 3, dashed line). The calculated relaxation rate for a Maxwellian distribution (Fig. 3, solid line) agrees reasonably well with the experimental points. At higher electron temperatures, above ~ 20 K (corresponding to an average electron energy of 2.6 meV), the experimental relaxation occurs even faster than the theoretical estimate.

One could argue that besides electron-phonon scattering there are a number of other processes contributing to the energy relaxation of a photoexcited-electron (hole) distribution: formation of free excitons from $e-h$ pairs, capture of electrons (holes) into localized impurity states to form neutral donors (acceptors), etc. Also, the radiative recombination by which the electron distribution is probed in our experiments does provide such an "extra" dissipation process. The latter process, however, is not very effective because of the long decay time of the (e, A^0) emission band (exceeding 10^{-7} sec) compared with the scattering times ($\leq 10^{-9}$ sec) involved in the acoustic-phonon processes. Although we cannot exclude the former mechanisms, it is likely that they are of minor importance in the electron temperature region around 20 K, since they affect predominantly low-energy electrons.⁴

B. Power-Balance Equation: Steady-State Case

Here we can assume *a priori* a Maxwellian distribution (this is justified by the experimental findings of Sec. IV). Under steady-state conditions the power transferred to the electron distribution by the excitation light must equal the total power loss of the electron system to the lattice, given by the sum of Eqs. (7)–(9), if there were no other dissipative processes besides the interaction with the lattice.

The electron generation rate g is given by

$$g = P(\hbar\omega V)^{-1}. \quad (11)$$

P is the total light power absorbed by the crystal, $\hbar\omega$ is the excitation light energy, and V is the excited volume, given by the product of the illuminated area times the electron penetration depth of Sec. III. Next we consider the energy transferred to the distribution *per photoexcited electron*. It is smaller than $\langle E_c \rangle_i$, the initial average energy of the photoexcited electrons (see Sec. III), because of the following: At energies $\langle E_c \rangle_i \approx 350$ meV, the electrons are scattered more likely by LO-phonons than by other electrons, provided the electron density is low enough.⁵ Since $n_e \leq 10^{15}$ cm $^{-3}$ in the experiments, this is true. We are only interested in those electrons which undergo an $e-e$ collision (and thus become energetically randomized), because the formulas derived above consider only the power loss of the randomized distribution. This condition is fulfilled by all electrons which have passed the initial LO-phonon "cascade" by emitting successively the maximum number (say m) of LO phonons and end up temporarily at an energy $\langle E_c \rangle_i - m\hbar\omega_{LO} = 17$ meV. (In our specific case $m = 9$.) At this energy their power loss to acoustic phonons is small compared to the energy rate exchanged in $e-e$ collisions. Therefore, the power per electron transferred to the equilibrium distribution by the exciting light is given by

$$\left\langle \frac{dE}{dt} \right\rangle \cong \langle \langle E_c \rangle_i - m\hbar\omega_{LO} \rangle g n_e^{-1}, \quad (12)$$

where n_e is the electron concentration.

To determine the dependence of n_e on g we performed measurements of the integrated (e, A^0) emission intensity J as a function of excitation light power and found $J \propto g^p$, p decreasing from 0.8 to 0.62 for g ranging from 5×10^{17} to 2×10^{22} cm $^{-3}$ sec $^{-1}$. In the range of electron temperatures considered here J is proportional to n_e .²⁴ A measurement of the decay time τ_0 of the (e, A^0) emission at $n_0 = 2 \times 10^{13}$ cm $^{-3}$ (see Sec. III) finally gives the relation

$$n_e = n_0 (\tau_0 / n_0)^p g^p \quad (13)$$

($\tau_0 = 3.1 \times 10^{-7}$ sec for sample *d* of Fig. 4). Equations (11)–(13) provide the relationship between the excitation-light power density (in W/cm 2) measured in the experiments—right-hand ordinate of Fig. 4—and the power $\langle dE/dt \rangle$ transferred per carrier to the randomized electron distribution—left-hand ordinate of Fig. 4.³¹

Now we can compare the theoretical results of Sec. V (Fig. 4, dashed curve) with the experimental data (Fig. 4, solid lines). The features of the experimental curves—a steep increase of $\langle dE/dt \rangle$ above a certain electron temperature, a slope

of ~ 11 in this region, below the kink a slope of $1.6 \dots 2.7$ —agree at least qualitatively with theory. The temperature T_e , however, where the kink occurs ranged from 13 to 20 K in the experiments, whereas theory predicts 32 K. This means that in the electron temperature range above ~ 16 K there exist effective energy relaxation mechanisms which tend to prevent a rise in electron temperature with increasing excitation power even before the influence of LO-phonon scattering in the high-energy tail of the distribution sets in.

This observation indeed is consistent with the findings in the transient experiments discussed above (Sec. V A). We must emphasize, however, that the data presented here are insufficient to specify the additional scattering process further. In the low-temperature region ($T_e \leq 10$ K) we find satisfactory agreement of the cw results with theory, which justifies the simplifications involved in the derivation of Eqs. (11)–(13), and the connection between the two ordinate scales in Fig. 4.³¹

Finally, we summarize briefly the considerations of this and Sec. V A concerning the sequence of events that a photoexcited initially “hot” electron undergoes in relaxing towards the conduction-band edge. The magnitude of electron concentrations obtained in our experiments ($2 \times 10^{11} \leq n_e \leq 1.2 \times 10^{14} \text{ cm}^{-3}$) causes the photoexcited electrons to lose energy *first* by successive emission of the maximum (i. e., energetically possible) number of LO phonons. During this stage of energy relaxation e - e collisions are not yet effective. After the initial LO-phonon cascade interelectronic collisions become dominant and randomize the distribution. The energy relaxation of this randomized distribution is then provided by acoustic phonon scattering and, of course, by optical phonon scattering in the high-energy tail of the distribution, if T_e is high enough [see Eqs. (7)–(9); Fig. 5, solid line].

In addition, there exist several other energy

dissipation processes of lesser effectiveness: capture of electrons into excitonic and impurity states and radiative recombination with holes. They remove the photoexcited electrons from the conduction band and thus determine the lifetime (or the steady-state concentration) of the free-electron population.

VI. SUMMARY

Experimental results of the energy relaxation of photoexcited hot carriers in GaAs under cold-lattice conditions have been presented. The electron distribution function was measured by analyzing the line shape of the (e, A^0) emission in high-purity samples. Two different situations, (i) transient relaxation process after pulsed photoexcitation and (ii) steady-state heating of the electron distribution by the excitation light, were investigated. The results are compared quantitatively with theoretical energy relaxation rates, calculated from the standard one-phonon scattering processes known from hot-electron and transport theory. Both experiments agree reasonably well with theory at electron temperatures below 16 K. The experiments indicate the existence of an additional energy relaxation process contributing effectively in the electron temperature range above 16 K. The measurements of the electron energy distribution functions demonstrate that interelectronic collisions randomize the electron energies completely, even in the case of the very low electron densities of the order of $2 \times 10^{11} \text{ cm}^{-3}$ which were realized in the experiments.

ACKNOWLEDGMENTS

The author would like to express his gratitude to E. Grobe and K.-H. Zschauer for providing the GaAs samples. Many thanks are due to J. C. McGroddy, T. N. Morgan, and O. Christensen for helpful discussions and comments on the manuscript.

[†]A project of the Sonderforschungsbereich

“Festkörperspektroskopie” Darmstadt-Frankfurt, financed by special funds of the Deutsche Forschungsgemeinschaft.

*Work partly done at IBM Watson Research Center, Yorktown Heights, N.Y. 10598.

[‡]Present address: IBM Watson Research Center, Yorktown Heights, N.Y. 10598.

¹H. Ehrenreich, Phys. Rev. **120**, 1951 (1960); H. Ehrenreich, J. Appl. Phys. Suppl. **32**, 2155 (1961).

²E. M. Conwell, in *Solid State Physics*, edited by H. Ehrenreich, F. Seitz, and D. Turnbull (Academic, New York, 1967), Suppl. **9**, Chap. 3.

³A. Zylberstein, Phys. Rev. **127**, 744 (1962); J. F. Palmier, Phys. Rev. **B 6**, 4557 (1972).

⁴M. Lax, Phys. Rev. **119**, 1502 (1960); G. Ascarelli and S. Rodriguez, Phys. Rev. **124**, 1321 (1961); Phys. Rev. **127**, 167 (1962); R. A. Brown and S. Rodriguez, Phys. Rev. **153**, 890 (1967).

⁵R. Stratton, Proc. R. Soc. A **242**, 355 (1957); R. Stratton, Proc.

R. Soc. A **246**, 406 (1958); see also Ref. 2, Chap. 2.

⁶D. L. Rode, Phys. Rev. **B 2**, 1012 (1970); D. L. Rode and S. Knight, Phys. Rev. **B 3**, 2534 (1971).

⁷D. J. Oliver, Phys. Rev. **127**, 1045 (1962); R. S. Crandall, Phys. Rev. **B 1**, 730 (1970); C. M. Wolfe, G. E. Stillman, and W. T. Lindley, J. Appl. Phys. **41**, 3088 (1970); D. Kranzer and G. Eberharter, Phys. Status Solidi **A 8**, K89 (1971).

⁸C. Benoit à la Guillaume and P. Lavallard, in *Radiative Recombination in Semiconductors, Seventh International Conference on the Physics of Semiconductors*, Paris, 1964 (Dunod, Paris, 1964), p. 53; A. Mooradian and H. Y. Fan, Phys. Rev. **148**, 873 (1966).

⁹A. Mooradian, in *Laser Handbook*, edited by F. T. Arrecchi and E. O. Schultz-DuBois, (North-Holland, Amsterdam, 1972), p. 1409, and references therein.

¹⁰Jagdeep Shah and R. C. C. Leite, Phys. Rev. Lett. **22**, 1304 (1969).

¹¹P. D. Southgate and D. S. Hall, Appl. Phys. Lett. **16**, 280 (1970); P. D. Southgate, D. S. Hall, and A. B. Dreeben, J. Appl.

Phys. **42**, 2868 (1971).

- ¹²S. J. Heising, S. M. Jarrett, IEEE J. Quantum Electron. **QE-7**, 205 (1971).
- ¹³R. Z. Bachrach, Rev. Sci. Instrum. **43**, 734 (1972).
- ¹⁴P. B. Coates, J. Phys. E **1**, 878 (1968); C. C. Davis and T. A. King, J. Phys. A **3**, 101 (1970).
- ¹⁵E. O. Kane, J. Phys. Chem. Solids **1**, 249 (1957).
- ¹⁶G. Dresselhaus, A. F. Kip, and C. Kittel, Phys. Rev. **98**, 368 (1955).
- ¹⁷P. Lawaetz, Phys. Rev. B **4**, 3460 (1971).
- ¹⁸R. Ulbrich, Phys. Rev. Lett. **27**, 1512 (1971).
- ¹⁹R. Ulbrich (unpublished results).
- ²⁰M. D. Sturge, Phys. Rev. **127**, 768 (1962).
- ²¹The influence of the space-charge layer arising from the different diffusion behavior of electrons and holes has been neglected. The associated field strengths are of the order of 100 V/cm at the highest electron concentration.
- ²²This is to be contrasted with the spectra published by Rossi *et al.* [Phys. Rev. Lett. **25**, 1614 (1970)], where the existence of two adjacent acceptor levels complicated the situation. All samples chosen for the present investigation showed only one type of shallow acceptor with a ground-state energy $E_A = 26.9$ meV, as deduced from our photoluminescence spectra with the band-gap value $E_g = 1.5192$ eV.
- ²³D. M. Eagles, J. Phys. Chem. Solids **16**, 76 (1960).
- ²⁴W. P. Dumke, Phys. Rev. **132**, 1998 (1963).
- ²⁵R. Dingle, Phys. Rev. **184**, 788 (1969).
- ²⁶W. Schairer and T. O. Yep, Solid State Commun. **9**, 421 (1971).
- ²⁷J. A. Rossi, C. M. Wolfe, G. E. Stillman, and J. O. Dimmock, Solid State Commun. **8**, 2021 (1970).
- ²⁸R. Ulbrich, thesis (Frankfurt am Main, 1972) (unpublished).
- ²⁹Here we consider only the electron energy region below $\hbar\omega_{LO}$. In the range of electron concentrations and temperatures being discussed, the electron population is nondegenerate.
- ³⁰Sh. M. Kogan, Fiz. Tverd. Tela **4**, 2474 (1962) [Sov. Phys.-Solid State **4**, 1813 (1963)].
- ³¹In Ref. 10 an attempt was made to relate $\langle dE/dt \rangle$, defined as the power per electron transferred to the equilibrium distribution by the exciting light, with the excitation light power by considering only the fraction of electrons at an energy $E = \langle E_c \rangle_i$ which exchanged energy with the electron distribution, i.e., did *not* emit a LO phonon first. In the case of low electron density (see Sec. V B), it follows from our considerations that this would be justified only in the special case where $\langle E_c \rangle_i \cong \hbar\omega_{LO}$. Hence for given P the value for $\langle dE/dt \rangle$ derived in Ref. 10 is generally not correct.